Proteomic and transcriptomic profiling reveal different aspects of aging in the kidney

Yuka Takemon[1], Joel M. Chick[2,3], Isabela Gerdes Gyuricza[1], Daniel A. Skelly[1], Olivier Devuyst[4], Steven P. Gygi[2], Gary A. Churchill[1], and Ron Korstanje[1*]

[1]The Jackson Laboratory, Bar Harbor, ME 04609 USA; [2]Harvard Medical School, Boston, MA 02115, USA; [3]VividionTherapeutics, San Diego, CA 92121, USA; [4]Institute of Physiology, University of Zurich, Zurich, Switzerland

***For correspondence:** ron.korstanje@jax.org

Abstract

The kidney is an excellent model for studying organ aging. Kidney function shows steady decline with age and is easy to assay using urine or blood samples. However, little is known about the molecular changes that take place in the kidney during the aging process. In order to better understand the molecular changes that occur with age, we measured mRNA and protein levels in 188 genetically diverse mice at ages 6, 12, and 18 months. We observed distinctive change in mRNA and protein levels as a function of age. Changes in both mRNA and protein are associated with increased immune infiltration and decreases in mitochondrial function. Proteins show a greater extent of change and reveal changes in a wide array of biological processes including unique, organ-specific features of aging in kidney. Most importantly, we observed functionally important age-related changes in protein that occur in the absence of corresponding changes in mRNA. Our findings suggest that mRNA profiling alone provides an incomplete picture of molecular aging in the kidney and that examination of changes in proteins is essential to understand aging processes that are not transcriptionally regulated.

Introduction

Aging is characterized by a decline in physiologic function of all organs and increasing rates of disease and mortality. Kidney function is affected early in the aging process and declines progressively with age. Decreased renal volume and the loss of functioning filtration units (PMID:3989190), lead to a decline in glomerular filtration rate of 5%-10% per decade after the age of 35 in humans [1]. It is relatively easy and non-invasive to measure functional changes of the kidney in blood and urine [2]. Moreover, kidney function significantly impacts age-related diseases in other organs including cognitive impairment [3]. These factors make the kidney an excellent model to study organ-specific aging.

While physiological changes in kidney function are well documented, relatively little is known about the underlying molecular processes that drive age-related loss of function. Molecular profiling of normal aging kidneys at different life stages is most readily carried out in a model organism. Previous molecular profiling studies of the aging kidney have been limited to microarray based gene expression assays in young versus old kidneys of mice and rats [4-5]. More recently, single cell transcriptional profiling of aging C57BL/6NJ mice has been reported for multiple tissues, including kidney [6]. When aging studies are carried out in single inbred strains, they may display specific and idiosyncratic patterns of aging and thus lack generalizability beyond the particular strain studied [7]. In order to capture the full range of pathologies associated with the aging kidney, a genetically diverse set of animals is required. In addition, previous studies have not attempted to relate transcriptional variation to changes in protein levels that are arguably more relevant to physiological aging.

Here we examine physiological kidney function together with mRNA and protein levels in male and female Diversity Outbred (DO) mice at ages 6, 12 and 18 months. The DO mice are a genetically diverse, outbred population derived from 8 founder strains that together contribute >50 million well-characterized variants [8]. Importantly, each DO animal is genetically unique and has the potential to reveal distinct age-related pathologies. This allows us to examine the common features of age-related change that are not specific to a single genetic background. Genetic variation will drive variation in mRNA and protein abundances for the majority of genes expressed in the kidney. This provides a unique opportunity to characterize the relationship between mRNA expression and protein levels and to examine how this relationship changes with age.

Results

Experimental design.

We carried out a cross-sectional aging study of ~600 DO mice including equal numbers of male and female mice that were aged to 6, 12, and 18 months (***Figure S1***). To evaluate kidney function, we successfully collected spot urine from 490 mice (141 at 6 months, 199 at 12 months, 150 at 18 months) and measured albumin, creatinine, and phosphate levels. We obtained flash frozen tissue from the right kidney of 188 randomly selected mice (30 males and 33 females at 6 months; 31 males and 31 females at 12 months; 34 males and 29 females at 18 months). The left kidney was collected and fixed for histology. We quantified mRNA by RNA-Seq and detected expression of 22,259 genes. We obtained untargeted proteomics data on the same set of 188 kidney samples and quantified 6,580 proteins representing 6,515 unique genes. Both mRNA and protein data were available for 6,449 genes.

Sources of variation in mRNA and protein expression.

In order to characterize the main sources of variation in mRNA and protein in aging mouse kidney, we computed principle components on the common set of 6,449 genes. Data were transformed to rank-normal scores to reduce the influence of outliers.

The top four principle components (PCs) for RNA explain 46.5% of variance (***Figure 1A***). The first PC explains 22.1% of variance and is strongly correlated with sex (p-value<2.2×10^{-16}) and only weakly correlated with age (p-value=0.050). The second PC (PC2) explains 15.3% of total variance and is not associated with sex (p-value=0.30) or with age (p-value=0.87). PC2 is explained by a batch effect in the RNA sequencing that we account for in subsequent analyses (see Materials and Methods). The effects of age on mRNA are apparent in the 3rd and 4th PCs but these explain 5% or less of total variation. Overall sex is a dominant factor in determining mRNA variation with minor contribution attributable to age.

The top four PCs for protein explain 39.1% of total variation (***Figure 1B***). The first PC explains 16.6% and is strongly associated with age (p-value=5.3×10^{-14}) but not with sex (p-value=0.24). The second PC explains 12.0% of variation. It is associated with sex (p-value<2.2×10^{-16}) and only marginally so with age (p-value=0.014). Effects of age and sex are apparent in the 3rd and 4th PCs which each explain less than 5% of total variation. In contrast to mRNA, age is a dominant factor in determining protein variation with lesser but still substantial influence due to sex. We also observed that the age-specific variability of the protein PCs (especially PC1 and PC4) is greater

in the 18-month animals indicating that there is greater between-animal variation in protein at later ages. In contrast, variation of mRNA is constant across age groups.

Age-related changes in mRNA expression.

To identify transcripts that change with age, we applied differential expression testing with DESeq2 [9] (see Materials and Methods) (***Table_S1***). We identified 449 transcripts that showed a trend with age (adjusted p-value<0.05) of which 426 show increasing expression with age and only 23 are decreasing. The mRNA species that increase with age include 83 immunoglobulin genes (Igh and Igk classes). Decreasing mRNA species include several that encode heat shock proteins (*Hsp90aa1*, *Hsp90ab1*, *Hsph1*, and *Hspa4l*).

We evaluated the list for functional enrichment of GO categories using ClusterProfiler [10] (***Figure 2***). We observed significant overrepresentation of genes associated with adaptive immune response (adjusted p-value=$1.3x10^{-23}$), leukocyte activation (adjusted p-value=$4.9x10^{-25}$), and leukocyte cell-cell adhesion (adjusted p-value=$1.4x10^{-16}$). All of the top 100 enrichment categories were related to immune cell functions. Increased expression of immune and inflammatory response genes in the aging kidney has been shown in previous mRNA expression studies and is likely the result of immune cell infiltration into the kidney [11-13].

In order to identify the cell-types involved in age related changes, we performed *in silico* cell type deconvolution of our bulk RNA-Seq data using published transcriptional profiles from single cell RNA-Seq data [14]. We found a significant increase in B cell proportion (adjusted p=$6.75x10^{-6}$) as well as macrophage proportion (adjusted p-value=0.0155) with age in both sexes (***Figure S2***).

Among the mRNA with most significant age-related changes, we noted increasing expression of *Cdkn2a* (adjusted p-value=$6.1x10^{-9}$) (***Figure S3A***). One of the two proteins encoded by *Cdkn2a*, p16 (or p16INK4a) is a hallmark for senescence [15]. However, due to low expression levels we were not able to quantify isoform-specific expression. In an in vivo study, *Cdkn2a* was found to be highly expressed in the renal cortex, and associated to severity of age-associated glomerulosclerosis, tubular damage and interstitial fibrosis [16-17]. We also observed increased expression of cyclin dependent kinase genes *Cdkn1a* and *Cdkn1c*. These genes play a role in DNA damage repair and regulation of apoptosis and cellular senescence. Increased expression of other markers of cellular senescence include *Mmp14* and *Mmp3* (***Figure S3C***).

Other genes of interest with respect to renal aging and decline are *Lcn2,* encoding Neutrophil Gelatinase-Associated Lipocalin (NGAL) (Figure S3D) and *Timp1*. In patients with Chronic Kidney Disease (CKD), NGAL closely reflects renal impairment and represents a strong and independent risk marker for progression of CKD [18]. TIMP-1 has been shown to promote age-related renal fibrosis [19].

Together these age-related changes in transcripts indicate infiltration of immune cells, increased cytokine activity, and cellular senescence.

Age-related changes in Protein Expression

We applied a linear mixed model ANOVA to protein abundance data after applying a rank-normal scores transformation and including covariates to account for marginal effects of peptide labeling tags, generation of DO mice, and sex. We identified 876 proteins that change with age (adjusted p-value<0.05) (***Table S2***). Of these, 352 increased with age and 524 decreased. Proteins with the most significant age trends include HIST1H1B and other histones that are decreasing with age; increasing ACTA2 a marker gene for myofibroblasts and indicator of renal fibrosis [20]; decreasing NCLN, which is part of a complex in the endoplasmic reticulum [21]; and decreasing CISD2, which is involved in mitochondrial autophagy [22] (***Figure S4***).

We evaluated the proteins for functional enrichment of GO categories using ClusterProfiler and observed overrepresentation of genes associated with 186 terms (adjusted p-value<0.01) representing a wide array of biological processes (***Figure S5A***), cellular compartments (***Figure S5B***), and molecular functions (***Figure S5C***). We observed a general pattern of decrease with age for protein associated with oxidative phosphorylation (adjusted p-value=$1.7x10^{-8}$) and the mitochondrial membrane (adjusted p-value=$2.2x10^{-12}$), as well as protein exit from the endoplasmic reticulum (adjusted p-value=$3.8x10^{-5}$), glycosylation (adjusted p-value=$2.6x10^{-4}$) and the endoplasmic reticulum membrane (adjusted p-value=$1.1x10^{-19}$). We observed an overall increase in genes associated with the actin cytoskeleton (adjusted p-value=$4.2x10^{-5}$).

We observed numerous changes, both increasing and decreasing with age, in proteins associated with transmembrane transport (adjusted p-value=$1.7x10^{-19}$) and the plasma membrane (adjusted p-value=$3.4x10^{-6}$). These proteins are associated with mitochondrial, endoplasmic reticulum, (Golgi and nuclear membranes) as well the plasma membrane. Many of the latter are markers of specific cell types in the kidney. In order to better understand the mixed patterns of change, we

identified genes from the enrichment categories that could be associated with specific cell types as well as the basal and apical cell surfaces of proximal tubule cells (***Figure 3***).

Two kidney-specific processes stand out: First, there is a large representation of transporters expressed in the proximal tubule cells. These are the most abundant cells in the renal tubule and do most of the work in reabsorbing salts, amino acids, glucose, and water, moving it from the filtrate back to the blood stream through transporters and channels on both the apical side and the basolateral side. Strikingly, we see a significant upregulation with age of the transporters on the apical side (e.g. SLC5A2 (or SGLT2), SLC7A9, SLC10A2, SLC5A8, and SLC6A19), while at the same time a significant downregulation of transporters on the basolateral side (e.g. SLC2A1 (a.k.a. GLUT1), SLC26A1, SLC4A4, SLC12A6, SLC12A7, SLC13A3, and SLC19A1). Interestingly, many of these basolateral transporters depend on ion gradients generated by the Na+/K+ ATP pump for their ability to function and both subunits of this pump (ATP1A1 and ATP1B1) are significantly decreased with age. A picture of reduced proximal tubular function is completed by the overall decrease in many mitochondrial proteins, including VDAC1, which is one of the key proteins that regulate mitochondrial function and is considered the gatekeeper for the passages of metabolites, nucleotides, and ions [23]. Transport requires a large amount of energy and proximal tubule cells are one of the most ATP-requiring cells and therefore a cell type with a very high mitochondrial content. We observe a decrease of proteins from all mitochondrial complexes as well as mitochondria-specific transporters.

The second important kidney-specific process that is suggested by the age-related changes in protein abundance is the actin remodeling in the podocytes. Remodeling of the actin cytoskeleton has a primary role in the structural adaptations made by these cells to preserve their glomerular filtration properties. Focal adhesions and slit diaphragms are signaling networks that interact with the actin cytoskeleton, maintain balance between intracellular and extracellular signals, and regulate podocyte function and morphology [24]. For the focal adhesions, we see a decrease in dystroglycan (DAG1), a protein that is highly abundant at the interface between the podocyte foot process and the glomerular basement membrane (GBM). The slit diaphragm contains proteins that include nephrin (NPHS1) and CD2AP, both increased with age, and they regulate Cofilin (CFL1) activity, which is also increased and leads to stabilization of the actin cytoskeleton. We see an increase in actinin 4 (ACTN4), which crosslinks actin filaments in the podocyte and interacts with various other proteins. Two other upregulated proteins linking to the actin filaments and involved in filament organization are MYO1C and MYO1E. Interesting, MYH9, which also

interacts with actin filaments to contract the cytoskeleton, is decreased with age. AKT2, encoding the RACβ serine/threonine-protein kinase, has an essential role in maintaining podocyte viability and normal cytoarchitecture after nephron loss [24]. We see that AKT2 is upregulated with age. Activation of AKT2 is mediated by mTOR complex 2. Overall, these changes with age suggest actin remodeling of the podocyte foot processes, which may be due to changes in glomerular filtration rate.

Overall, we see that proteomics reveals a highly varied array of both fundamental and kidney-specific changes that are occurring at the cellular level. The picture that emerges is distinct and complementary to age-related changes observed at the transcriptional level.

Comparison of Age-related changes in mRNA and Protein

In order to compare age-related trends in mRNA and proteins, we identified 6,514 proteins (representing 6,449 distinct genes) that had corresponding mRNA data. For purposes of this analysis, we applied a more liberal false discovery rate (FDR<0.1) multiple test correction. To provide a point of reference for interpreting the age comparisons we also compared mRNA and protein difference between the sexes.

We identified significant (FDR<0.1) age trends in 1493 mRNAs and 3,871 proteins. Direct comparison of the numbers of statistically significant mRNA and protein species that are changing with age is complicated by the potential difference in precision of the measurements as well as the different statistical testing methods. However, applying the same statistical criteria, we identified 5325 mRNAs and 4412 proteins with significant sex-specific differences. This suggests that we are not underpowered to detect changes in mRNA. We conclude that age-related changes are more prevalent for proteins as compared to mRNA, consistent with our analysis of the principle components of variation described above.

We looked at concordance in the directions of change between mRNA and protein. The absolute units of change are difficult to compare directly so we converted the estimated fold-change (mRNA) or trend (protein) to z-scores (estimate/standard error). The correlation of age-trends between mRNA and protein ($r=0.235$, p-value$<2.2\times10^{-16}$) is positive and highly significant but much smaller than the correlation of sex-specific differences ($r=0.626$, p-value$<2.2\times10^{-16}$). We identified genes for mRNA and protein with age-trends that are concordant increasing (Group A, n=309), discordant with mRNA decreasing and protein increasing (Group B, n=196), discordant

with mRNA increasing and protein decreasing (Group C, n=108), and concordant decreasing (Group D, n=359) (***Figure 4A***). There are more genes with concordant changes (10.3%) but a substantial proportion of genes have changes with age occur in opposite directions (4.7%). We classified sex-specific differences according to direction of change (F>M or F<M) and found 1545, 153, 610, and 1391 genes in categories A-D, respectively. Sex-specific differences are much more likely to be concordant (42.7%) with a relatively smaller proportion of discordant genes (11.7%) (***Figure 4B***).

We applied functional enrichment analysis to each group of genes defined by concordant or discordant directions of change with age (***Table S3***).

Among the 309 genes with age-related increase in both mRNA and protein (Group A), the top enrichment categories are dominated by genes involved in the immune response, actin cytoskeleton organization, and cell adhesion. As with our analysis of mRNA changes above, this likely reflects increased infiltration of immune cells into the kidney that has been previously reported in both humans and rodents [11-12]. Other genes in this group include *Slc34a2*, which encodes a sodium-dependent phosphate transporter and *Nphs1*, encoding the podocyte slit-diaphragm structural component Nephrin. We also observed concordant increases in the immuno-proteosome complex (e.g., *Psmb8*, *Psmb9*, *Psmb10*, *Psme1*).

Among the 359 genes with concordant age-related decrease in mRNA and protein (Group D) we see enrichment of genes involved in transmembrane transport, mitochondrial membrane, Golgi vesicle transport that were noted previously. We also see enrichment of genes involved in junction formation including cadherins (*Cdh16*), catenins (*Ctnnb1,* and *Ctnnd1*) and claudins (*Cldn8*, *Cldn10*). Cell-cell junctions are important in kidney function as much of tubular transport depends on limiting the passage of molecules and ions through the space between cells. Several adhesion related genes such as *Aplp2* and *Ppfia1* have previously been associated with significant age-associated changes [11]. Although there is no direct evidence in the kidney, it has been shown that these junctions become leaky with age in other tissues [25].

Several proteins in ubiquitin mediated protein catabolism are concordantly downregulated (*Ubac2, Ube3c, Ubqln4, Ubr4, Usp20, Usp32, Usp33, Usp34, Usp39,* and *Usp9x*). Notable among the genes in this category is *Klotho*, an aging-suppressor gene primarily expressed in the kidney. *Klotho* is associated with fibrosis and is an antagonist of beta catenin [26]. Previous studies have shown that *Klotho* knockout mice exhibit increased incidence of aging-related diseases including

atherosclerosis, vascular and tissue calcification, and chronic kidney disease [17,27]. Decreased *Klotho* expression has been shown to drive accelerated aging [28] and renal failure [26].

We observed discordant age trends between mRNA and protein for a substantial number of genes. We identified 196 genes with decreasing mRNA and increasing protein levels with age (Group B). This group includes genes that are exclusively localized to the brush border of the proximal tubule (e.g., *Slc26a6*, *Slc34a3*, *Slc5a2*, *Slc3a1*, *Slc9a3*, *Pdzk1* and *Lrp2*) and are important for the reabsorption of specific metabolites in the ultrafiltrate. The glucose transporter SGLT2 (encoded by *Slc5a2*) is responsible for 97% of glucose reabsorption [29]. SLC3A1 and SLC7A9 together form the antiporter that mediates uptake of cysteine, which is of particular interest because of the potential role of cysteine in aging [30]. *Lrp2* encodes Megalin, the receptor that exclusively mediates albumin reabsorption in the proximal tubule and can affect the amount of albumin in the urine (see below). PDZK1 is a scaffold protein that connects membrane proteins and regulatory components at the apical side and has been shown to interact with several transporters in Group B, such as *Slc9a3* encoding the main sodium-hydrogen antiporter NHE3), responsible for sodium balance [31], *Slc22a6*, encoding OAT1, which plays a central role in organic anion transport, and *Slc34a1* and *Slc34a3*, encoding transporters important for phosphate transport (see below) [32].

We identified 109 genes with increasing mRNA and decreasing protein (Group C). This group is highly enriched for cytosolic ribosome including >20 genes from both small and large subunits. Group C also includes genes *Srsf3*, *Srsf5*, *Srsf6,* and *Snrpa1,* that are involved in RNA splicing. Age-related changes in alternative splicing has been implicated in contributing to the dysregulation of gene expression with aging. Down regulation of splicing factor, SRSF3, has been shown to induce alternative splicing of TP53 that results in cellular senescence [33]. It is interesting to note that for these aforementioned post-transcriptional processes, the direction of change differs between mRNA and proteins. Thus, hinting at possible age-related post-transcriptional regulation mechanisms at play.

Within each age category the correlations of mRNAs with their corresponding proteins are predominantly positive. Thus, the two groups of genes that show opposite directions of age-related change between mRNA and protein appear at first to present a paradox [34]. For example, *Slc5a12,* a gene that encodes a sodium-coupled lactate transporter in the proximal tubule (Group D), shows a significant decrease in mRNA and increase in protein levels with age (***Figure 5A***).

However, within each age group, we observe a positive correlation between mRNA expression and protein expression. *Flot1,* a gene in Group C, illustrates the opposite pattern of change (***Figure 5B***).

In order to further clarify the role of transcriptional regulation in determining age-related changes in protein, we carried a mediation analysis between protein and its corresponding mRNA for 6,667 genes. We evaluated the significance of the age trend in all proteins with and without accounting for changes in mRNA (***Figure 6A***). If age-related changes in protein are driven by corresponding changes in mRNA, we would expect age~protein correlations to drop after accounting for mRNA. However, we observe essentially no change in the significance of correlations and conclude that the age-related components of change in protein abundance occur independently of the mRNA. To provide a point of reference for interpreting the age mediation analysis, we repeated the same exercise with sex as the variable of interest (***Figure 6B***). These results suggest a very different mode of regulation of proteins that show sex-specific differences, i.e., differences in protein abundances between the sexes is a direct consequence of differences in mRNA abundance.

For many proteins, the level of RNA expression is a major determinant of the amount of its protein product that is present. However. the age-related changes in protein amounts are not driven by a corresponding age-related change in their mRNA. Rather, what appears to be changing with age is the relative abundance of protein for a given level of mRNA expression. This suggests that the processes that drive age-related change in proteins are post-translational and may involve specific changes in translational efficiency [35] or rates of mRNA or protein turnover [36].

Relating mRNA and Protein Changes to Physiology

Regulation of urinary filtrates is a critical function of the kidney to maintain adequate concentrations in the circulating serum. Here we examine the relations of genes that were identified with significant age-related changes in both mRNA and protein levels with urinary phenotypes in order to draw further insights into the biological mechanisms underlying renal aging.

The protein most strongly correlated with urinary phosphate is *Pdzk1ip1* (r=0.322, p-value=7.5x10^{-5} adjusted for sex; r=0.32, p-value=0.0027 adjusted for sex and age) (***Figure 7A***). *Pdzk1ip1* is expressed specifically in proximal tubule cells in segment S2 [37]. It interacts with *Pdzk1*, which is responsible for establishing a scaffolding in the brush border of proximal tubule

cells to anchor transporters and other membrane bound proteins [38]. *Pdzk1* and *Pdzk1ip1* are both Group B genes whose RNA decreases, and protein increases with age (***Figure 8A and B***). We fit a multivariable regression model to urinary phosphate and noted that after accounting for Pdzk1ip1 protein levels, age is no longer a significant predictor of urinary phosphate (p-value for age is 0.22 adjusted for PDZK1IP1). This is consistent with a causal for *Pdzk1ip1* as a mediator (or a close surrogate) for the change in urinary phosphate levels with age. We examined the set of 799 proteins that are significantly correlated with *Pdzk1ip1* (adjusted p-value<0.05) and found these to be enriched for membrane transporters and other proteins associated with the brush border and apical side of the cell (***Figure S6***). Interestingly, protein levels of NPT2A (*Slc34a1*) and NPT2C (*Slc34a3*) that form the major sodium-phosphate co-transporter do not correlate with urinary phosphate excretion (***Figure 7B and C***), confirming that phosphate reabsorption by this transporter is not regulated by the protein level of the subunits and instead by their interactions with PDZK1 and PDZK1IP1 [39].

Megalin, the protein encoded by *Lrp2*, is the receptor that mediates albumin reabsorption in the proximal tubule. It is another Group B gene that shows a decrease in both mRNA expression (p=value=2.4×10^{-5}), an increase in protein level (p-value=0.0043) with age and a positive correlation between mRNA and protein levels within each age group (***Figure 8C***). Megalin reabsorbs albumin that has passed through the glomerular basement membrane. The majority of animals in our DO cohort do not show albuminuria - 157 of the 188 animals had albumin levels below 1 mg/dL – and although this limits our ability to draw conclusions regarding the relationship between urinary albumin levels and Megalin expression levels – Megalin is negatively correlated with albumin (p-value=0.081 after regression adjustment for sex and age) (***Figure 7D***).

Discussion

The kidney is an excellent model for studying organ-specific aging. Its function is relatively easy to measure (through blood and urine) and functional changes can be observed early in the aging process. Although molecular changes in the aging kidney have been studied previously, these have been limited to microarray assays and RNAseq of mRNA expression. An implicit assumption of these studies is that changes in gene function (protein levels) can be extrapolated from changes in mRNA. While other have reported that mRNA can be a poor proxy for protein abundance [40], we find that the direction of change of a protein with age cannot be reliably predicted based on changes in its coding mRNA even for genes where the mRNA and protein are correlated within

age groups. We were able to confirm previously reported transcriptional changes in the kidney with age, such as the increase in immune related pathways due to immune cell infiltration. However, in this study we provide another layer of understanding through our data that show that the changes in the aging kidney at the molecular level are more complicated than a change in gene expression directly affecting the expression of the encoded protein in the same direction. In fact, in most cases, at the global level we show that the changes in protein expression related to aging are not mediated through mRNA levels. Through distilling this global information, we were able to obtain valuable information that distinctly show that changes in mRNA and protein can shift in both concordant and discordant direction and are pathway and cell-type dependent.

Many mechanisms known to affect the aging process can explain this disconnect between mRNA expression and protein expression. Gene-specific changes in translation rate may cause these differences. However, a recent study in which RNAseq and Riboseq data was compared in kidneys in 3, 20, and 32-month old male C57BL/6 mice concluded no significant changes in translation rates between time points [35]. Loss of proteostasis is a hallmark of aging that manifests at the cellular level in a number of ways, such as protein aggregation, unfolding, oxidative damage, post-translational modification and altered rates of protein turnover [41]. We recently found a decrease in correlation between protein subunits of the 26S proteasome complex in the heart of DO mice with age, suggesting that loss of stoichiometry of the proteasome system itself may contribute to the decline in the protein quality control process during aging [42]. Since proteostasis is tailored to the specific proteomic demands of different cells and the kidney consists of many different cell types, this is difficult to entangle in our study. Furthermore, our study can only detect protein levels and we cannot draw any conclusions about the status of the protein (functional, modified, or damaged). However, the significant changes in a number of ubiquitin-related genes and enrichment of proteins associated with the membrane of the endoplasmic reticulum with age may suggest important roles for these parts of the proteostasis network.

It is important to note that protein abundance does not equal protein function. In our study, the observation that proximal tubule specific transporters on the apical side are increased with age, while at the same time transporters at the basolateral side are decreased poses the question what happens to cellular transport. However, increased apical-associated transporters does not necessarily mean increased uptake of molecules from the lumen and a build-up of these molecules in the cell as the transporters may not be localized to the brush border.

In conclusion, there appear to be distinct modes of aging when comparing the transcriptome and the proteome in the mouse kidney and that changes with age at the mRNA and protein level are driven by different factors. Identifying these factors and the mechanisms that disconnect gene expression from protein expression at the global scale with age will be essential to understand what drives the kidney (and possibly other organs) to become more susceptible to disease with age and to develop novel therapies to build resilience against them.

Age related changes in protein levels are not driven by corresponding changes in mRNA. Instead they reflect a change in the balance of protein homeostasis that is altered in older animals compared to young animals. The global pattern of genetic regulation of age-specific changes is distinct from the genetic regulation of sex differences in protein levels which appear to be largely driven by corresponding changes in mRNA. Our finding indicate that changing protein homeostasis is aging animals occurs as a result of changes in post-transcriptional processes – through changes in translation efficiency or of protein turnover. These changes are likely coordinated across functionally related groups of genes.

Materials and Methods

Study cohort

Our initial cohort consisted of 600 Diversity Outbred mice (300 males and 300 females) bred at The Jackson Laboratory (stock no. 009376) in 5 breeding waves (generations 8, 9, 10, 11, and 12). 100 males and 100 females were randomly assigned to each of three groups for which tissues were collected at 6, 12, and 18 months of age. Animals were maintained on a standard rodent diet (LabDiet 5K52, St. Louis, MO, USA) in an animal room free of pathogens, at a temperature between 20 and 22 ºC, and a 12-hour light:dark cycle. At the selected ages, urine samples were collected, the right kidney was flash-frozen. Urinary albumin, phosphate, and creatinine were measured on a chemistry analyzer (Beckman Coulter AU680, Brea, CA, USA). For 188 samples, equally distributed by age and sex, flash-frozen kidney samples were pulverized and aliquoted for RNA-seq and shotgun-proteomic analysis. The Jackson Laboratory's Institutional Animal Care and Use Committee approved all reported mouse studies.

DNA isolation and Whole-genome diplotype probability construction

Tail tips were collected and DNA was isolated using standard methods. DNA concentration and purity were measured using a NanoDrop 2000 spectrophotometer (Thermo Fisher Scientific,

Waltham, MA, USA). Samples met stringent quality standards of A260/280 ratio between 1.7 and 2.1. Mice were fully genotyped for 78,000 SNPs using the GeneSeek Mega Mouse Universal Genotyping Array (MegaMUGA) (Neogen Genomics, Lincon, NE, USA) [43]. Founder haplotype mosaics were reconstructed using a Hidden Markov Model of array intensity data generated from the BeadStudio (Illumina, San Diego, CA, USA) algorithm. To ensure quality of genotype construction, samples with call rates of 90% and over were kept.

Total RNA isolation and quality control

The pulverized whole kidney samples were lysed and homogenized in Ambion TRIzol reagent (Thermo Fisher Scientific #15596026). Total RNA was isolated using miRNeasy Mini kit (Qiagen Inc. #217004, Germantown, MD, USA) according to manufactures' protocols, including the optional DNase digest step. Sample concentration and quality were assessed using the Nanodrop 2000 spectrophotometer and RNA 600 Nano LabChip assay (Aligent Technologies, Santa Clara, CA, USA).

Library construction and High-throughput RNA sequencing

Poly(A) RNA-seq libraries were constructed using the TruSeq RNA Library Prep Kit v2 (Illumina), including the addition of unique barcode sequences. Library quality and quantity were assessed using the DNA 1000 LabChip assay (Agilent Technologies) and quantitative PCR (Kapa Biosystems, Wilmington, MA, USA). 8 pools of 24 randomized libraries were sequenced in 3 lanes at 100 bp single-end on the HiSeq 2500 (Illumina) using TruSeq SBS Kit v4 reagents (Illumina).

High-throughput proteomics

Samples of the same mice that were used for RNA-seq were homogenized in 1 ml lysis buffer, which consists of 1% SDS, 50 mM Tris, pH 8.8 and Roche cOmplete protease inhibitor cocktail (Roche # 11697498001, Clifton, NJ, USA), and analyzed as previously described (PMID:27309819)

Quantification and testing of RNA-seq data

Genotyping By RNA-Seq software (https://gbrs.readthedocs.io/en/latest/) was used to align the RNA-Seq reads and reconstruct the individual haplotypes of DO mice. GBRS-constructed haplotypes were cross-compared against MegaMUGA-constructed diplotypes as a confirmation step to identify and correct sample mix-ups [44]. We applied Expectation-Maximization algorithm for Allele Specific Expression (EMASE) [45] to quantify gene expression from the individual

aligned RNA-seq data. Count data were normalized using DESeq2 [9] variance stabilizing transformation. Differential expression testing was done with DESeq2 using a likelihood ratio test to evaluate changes with age (as a linear trend) after accounting for sex and sequencing batch.

Quantification and testing of Protein expression data

Tissue from the total (right) kidney samples were homogenized in 1 ml lysis buffer, which consisted of 1% SDS, 50 mM Tris, pH 8.8 and Roche complete protease inhibitor cocktail (Roche # 11697498001, Clifton, NJ, USA), and analyzed as previously described [46]. Protein abundances were estimated from their component peptides identified through mass-spectrometry (MS) followed by a database search of MS spectra. Prior to protein expression estimation, we filtered out peptides that contained polymorphisms relative to the mouse reference genome. We determined the age-related changes for each protein by computing the likelihood ration test for age (as a linear trend) using a mixed model linear regression with random effect terms to account for protein labeling (Tag), DO mouse generation, and a fixed-effect correction for sex. The regression coefficient and p-values generated from this model was used to determine the significant change in direction of the mRNA and proteins.

For both mRNA and protein data, we applied two types of multiple test corrections. We applied a stringent family-wise error correction using Holm's method (https://www.jstor.org/stable/4615733), indicated as "adjusted p" in the text. We applied a less stringent false discovery rate correction using the Benjamini-Hochberg method (http://www.jstor.org/stable/2346101), indicated as "FDR" in the text.

***In silico* cell type deconvolution of bulk RNA-Seq**

In order to examine relative changes in cell composition with age, we used *in silico* cell type deconvolution as implemented in the CellCODE R package [47]. This approach uses marker genes derived from transcriptional profiles ascertained for purified cell types to quantify changes in cell composition in a heterogeneous mixture of RNA (bulk RNA-Seq). For this analysis we used a bulk gene expression matrix that was upper quartile normalized to account for differences in library size. We obtained cell type-specific transcriptional profiles using single cell RNA-Seq data and cell type labels from Park et al. [14]. To obtain markers from single cell transcriptional profiles, we normalized the count matrix by the number of unique molecular identifiers (UMI) per cell per ten thousand UMIs, took the log of counts + 1, and calculated mean expression of each gene in each cell type. We allowed up to 50 markers per cell type and calculated surrogate proportion

variables using the "raw" method to ensure that trends in relative cell type proportions were estimated independently of mouse age [47].

Mediation analysis

mRNA expression as a predictive mediator to the changes in protein expression driven by age and sex was investigated by comparing p-values generated from calculating linear regression models with and without mediation. The unmediated model accounted from changes in protein caused by Age or Sex and DO generation ($Protein_i \sim Age_i/Sex_i + Generation_i$), and the mediated model accounted for the corresponding mRNA expression as an additional covariate in the linear regression model ($Protein_i \sim Age_i/Sex_i + Generation_i + mRNA_i$).

Data normalization and statistics

All RNA-seq expression data and proteomics data were transformed to rank-normal scores [48] prior to analysis, unless otherwise stated. Albumin and urinary phosphorus data were log transformed after regression adjustment for urinary creatinine levels. Data analysis and figures were generated using R v4.0.0.

Data access

Source data and analysis scripts have been deposited with FigShare (reference # pending). In addition, the transcript and protein data are available in an online tool that supports genetic mapping analysis (https://churchilllab.jax.org/qtlviewer/JAC/DOKidney).The RNA-seq data have been deposited in NCBI's Gene Expression Omnibus, accession number GSE121330 (https://www.ncbi.nlm.nih.gov/geo/query/acc.cgi?acc=GSE121330). The proteomics data have been deposited in PRIDE proteomic repository (reference # pending).

Acknowledgements

We gratefully acknowledge the contribution of Heidi Munger and the Genome Technologies Service at The Jackson Laboratory for expert assistance with the work described in this publication. This work was supported by the National Institutes of Health grant to The Jackson Laboratory Nathan Shock Center of Excellence in the Basic Biology of Aging (AG038070).

Author contributions

RK, GC and SG conceived, and designed the experiments. YT, RK and GC wrote the manuscript. YT prepared the kidneys for RNA-seq and shotgun proteomics. JC and SG carried out the mass-spec proteomics experiments. YT and GC analyzed the data. IG contributed to the data analysis. OD generated the urinalysis data. DS conducted *in silico* cell type deconvolution analysis of the RNA-seq data.

Figures and Tables

Figure 1. Principal component analysis. The top four principle components for (A) RNA, with sex as the dominant factor and (B) protein, with age as the dominant factor.

Figure 2. Analysis of differentially expressed mRNA with age. (A)Functional enrichment and (B) network analysis shows overrepresentation of genes involved in immune and inflammatory response and is likely the result of immune cell infiltration into the kidney.

Figure 3. A subset of differentially expressed proteins with age that are specific for various parts of the nephron show distinct changes with age, such as actin-cytoskeleton rearrangement in podocytes and changes in proximal tubular transport.

Figure 4 Comparison of age-related changes in mRNA and protein. We identified 6,514 genes with both mRNA and protein data of which 972 had significant differences with age for both mRNA and protein. These can be divided in 4 groups depending on the direction of change (A). There is a similar pattern for sex-specific differences, although these are much more likely to be concordant (B).

Figure 5 Examples of genes with opposite directions of age-related changes between mRNA and protein. (A) *Slc5a12* shows a decrease in mRNA and an increase in protein with age. Within age groups there is a positive correlation between mRNA and protein expression, but comparison between time points. (B) *Flot1* shows the opposite with increased mRNA and decreased protein with age.

Figure 6. Age-related changes in protein expression are not mediated by mRNA expression.

Figure 7. Correlation with phosphate and albumin (normalized to creatinine). (A) PDZK1IP1 is the protein with the highest correlation with urinary phosphate levels and mediation analysis suggests the protein is a mediator for changes in urinary phosphate levels. There are no significant correlations for phosphate with SLC34A1 (B) or SLC34A3 (C) that form the main phosphate transporter in the proximal tubule. (D) Significant correlation between albumin and its proximal tubule receptor Megalin (LRP2).

Figure 8. *Pdzk1* (A), *Pdzk1ip1* (B), and *Lrp2* (C) are genes with decreased mRNA and increased protein expression with age.

Figure S1. Experimental Design

Figure S2. In silico cell type deconvolution of bulk RNA-seq data.

Figure S3. Examples of differential mRNA expression with age

Figure S4. Examples of differential protein expression with age

Figure S5. Functional enrichment of differentially expressed proteins and networks

Figure S6. Protein Cnet plots

Table S1. List of genes with significant age-related, sex-related, and age-by-sex interaction-related changes in mRNA expression levels.

Table S2. List of genes with significant age-related, sex-related, and age-by-sex interaction-related changes in protein expression levels.

Table S3. List of genes with significant age-associated changes in both mRNA and protein levels and their direction of change.

Table S4. List of genes with significant sex-associated changes in both mRNA and protein levels and their direction of change.

References

[1] Glassock, R., Rule, A. (2012). The implications of anatomical and functional changes of the aging kidney: with an emphasis on the glomeruli Kidney International 82(3), 270 - 277. https://dx.doi.org/10.1038/ki.2012.65

[2] Lindeman, R., Tobin, J., Shock, N. (1985). Longitudinal Studies on the Rate of Decline in Renal Function with Age Journal of the American Geriatrics Society 33(4), 278-285. https://dx.doi.org/10.1111/j.1532-5415.1985.tb07117.x

[3] Elias, M., Elias, P., Seliger, S., Narsipur, S., Dore, G., Robbins, M. (2009). Chronic kidney disease, creatinine and cognitive functioning Nephrology Dialysis Transplantation 24(8), 2446-2452. https://dx.doi.org/10.1093/ndt/gfp107

[4] Jonker, M., Melis, J., Kuiper, R., Hoeven, T., Wackers, P., Robinson, J., Horst, G., Dollé, M., Vijg, J., Breit, T., Hoeijmakers, J., Steeg, H. (2013). Life spanning murine gene expression profiles in relation to chronological and pathological aging in multiple organs Aging Cell 12(5), 901-909. https://dx.doi.org/10.1111/acel.12118

[5] Park, D., Kim, B., Kim, C., Choi, Y., Jeong, H., Kim, M., Lee, J., Park, M., Chung, K., Kim, D., Lee, J., Im, D., Yoon, S., Lee, S., Yu, B., Bhak, J., Chung, H. (2016). RNA-Seq analysis reveals new evidence for inflammation-related changes in aged kidney Oncotarget 7(21), 30037-30048. https://dx.doi.org/10.18632/oncotarget.9152

[6] Almanzar, N., Antony, J., Baghel, A., Bakerman, I., Bansal, I., Barres, B., Beachy, P., Berdnik, D., Bilen, B., Brownfield, D., Cain, C., Chan, C., Chen, M., Clarke, M., Conley, S., Darmanis, S., Demers, A., Demir, K., Morree, A., Divita, T., Bois, H., Ebadi, H., Espinoza, F., Fish, M., Gan, Q., George, B., Gillich, A., Gòmez-Sjöberg, R., Green, F., Genetiano, G., Gu, X., Gulati, G., Hahn, O., Haney, M., Hang, Y., Harris, L., He, M., Hosseinzadeh, S., Huang, A., Huang, K., Iram, T., Isobe, T., Ives, F., Jones, R., Kao, K., Karkanias, J., Karnam, G., Keller, A., Kershner, A., Khoury, N., Kim, S., Kiss, B., Kong, W., Krasnow, M., Kumar, M., Kuo, C., Lam, J., Lee, D., Lee, S., Lehallier, B., Leventhal, O., Li, G., Li, Q., Liu, L., Lo, A., Lu, W., Lugo-Fagundo, M., Manjunath, A., May, A., Maynard, A., McGeever, A., McKay, M., McNerney, M., Merrill, B., Metzger, R., Mignardi, M., Min, D., Nabhan, A., Neff, N., Ng, K., Nguyen, P., Noh, J., Nusse, R., Pálovics, R., Patkar, R., Peng, W., Penland, L., Pisco, A., Pollard, K., Puccinelli, R., Qi, Z., Quake, S., Rando, T., Rulifson, E., Schaum, N., Segal, J., Sikandar, S., Sinha, R., Sit, R., Sonnenburg, J., Staehli, D., Szade, K., Tan, M., Tan, W., Tato, C., Tellez, K., Dulgeroff, L., Travaglini, K., Tropini, C., Tsui, M., Waldburger, L., Wang, B., Weele, L., Weinberg, K., Weissman, I., Wosczyna, M., Wu, S., Wyss-Coray, T., Xiang, J., Xue, S., Yamauchi, K., Yang, A., Yerra, L., Youngyunpipatkul, J., Yu, B., Zanini, F., Zardeneta, M., Zee, A., Zhao, C., Zhang, F., Zhang, H., Zhang, M., Zhou, L., Zou, J. (2020). A single-cell transcriptomic atlas characterizes ageing tissues in the mouse Nature 583(7817), 590-595. https://dx.doi.org/10.1038/s41586-020-2496-1

[7] Voelkl, B., Altman, N., Forsman, A., Forstmeier, W., Gurevitch, J., Jaric, I., Karp, N., Kas, M., Schielzeth, H., Casteele, T., Würbel, H. (2020). Reproducibility of animal research in light of biological variation. Nature reviews. Neuroscience https://dx.doi.org/10.1038/s41583-020-0313-3

[8] Svenson, K., Gatti, D., Valdar, W., Welsh, C., Cheng, R., Chesler, E., Palmer, A., McMillan, L., Churchill, G. (2012). High-resolution genetic mapping using the Mouse Diversity outbred population. Genetics 190(2), 437 - 447. https://dx.doi.org/10.1534/genetics.111.132597

[9] Love, M., Huber, W., Anders, S. (2014). Moderated estimation of fold change and dispersion for RNA-seq data with DESeq2 Genome Biology 15(12), 550. https://dx.doi.org/10.1186/s13059-014-0550-8

[10] Yu, G., Wang, L., Han, Y., He, Q. (2012). clusterProfiler: an R Package for Comparing Biological Themes Among Gene Clusters OMICS: A Journal of Integrative Biology 16(5), 284-287. https://dx.doi.org/10.1089/omi.2011.0118

[11] Rodwell, G., Sonu, R., Zahn, J., Lund, J., Wilhelmy, J., Wang, L., Xiao, W., Mindrinos, M., Crane, E., Segal, E., Myers, B., Brooks, J., Davis, R., Higgins, J., Owen, A., Kim, S. (2004). A Transcriptional Profile of Aging in the Human Kidney PLoS Biology 2(12), e427. https://dx.doi.org/10.1371/journal.pbio.0020427

[12] Melk, A., Mansfield, E., Hsieh, S., Hernandez-Boussard, T., Grimm, P., Rayner, D., Halloran, P., Sarwal, M. (2005). Transcriptional analysis of the molecular basis of human kidney aging using cDNA microarray profiling Kidney International 68(6), 2667-2679. https://dx.doi.org/10.1111/j.1523-1755.2005.00738.x

[13] Park, D., Kim, B., Kim, C., Choi, Y., Jeong, H., Kim, M., Lee, J., Park, M., Chung, K., Kim, D., Lee, J., Im, D., Yoon, S., Lee, S., Yu, B., Bhak, J., Chung, H. (2016). RNA-Seq analysis reveals new evidence for inflammation-related changes in aged kidney Oncotarget 7(21), 30037-30048. https://dx.doi.org/10.18632/oncotarget.9152

[14] Park, J., Shrestha, R., Qiu, C., Kondo, A., Huang, S., Werth, M., Li, M., Barasch, J., Susztak, K. (2018). Single-cell transcriptomics of the mouse kidney reveals potential cellular targets of kidney disease. Science 360(6390), 758 - 763. https://dx.doi.org/10.1126/science.aar2131

[15] Hernandez-Segura, A., Nehme, J., Demaria, M. (2018). Hallmarks of Cellular Senescence Trends in Cell Biology 28(6), 436-453. https://dx.doi.org/10.1016/j.tcb.2018.02.001

[16] Melk, A., Schmidt, B., Vongwiwatana, A., Rayner, D., Halloran, P. (2005). Increased Expression of Senescence-Associated Cell Cycle Inhibitor p16INK4a in Deteriorating Renal Transplants and Diseased Native Kidney American Journal of Transplantation 5(6), 1375-1382. https://dx.doi.org/10.1111/j.1600-6143.2005.00846.x

[17] Bolignano, D., Mattace-Raso, F., Sijbrands, E., Zoccali, C. (2014). The aging kidney revisited: A systematic review Ageing Research Reviews 14(), 65-80. https://dx.doi.org/10.1016/j.arr.2014.02.003

[18] Bolignano, D., Lacquaniti, A., Coppolino, G., Donato, V., Campo, S., Fazio, M., Nicocia, G., Buemi, M. (2009). Neutrophil Gelatinase-Associated Lipocalin (NGAL) and Progression of Chronic Kidney Disease Clinical Journal of the American Society of Nephrology 4(2), 337-344. https://dx.doi.org/10.2215/cjn.03530708

[19] Zhang, X., Chen, X., Hong, Q., Lin, H., Zhu, H., Liu, Q., Wang, J., Xie, Y., Shang, X., Shi, S., Lu, Y., Yin, Z. (2006). TIMP-1 Promotes Age-Related Renal Fibrosis Through Upregulating ICAM-1 in Human TIMP-1 Transgenic Mice The Journals of Gerontology: Series A 61(11), 1130-1143. https://dx.doi.org/10.1093/gerona/61.11.1130

[20] Duffield, J. (2014). Cellular and molecular mechanisms in kidney fibrosis Journal of Clinical Investigation 124(6), 2299-2306. https://dx.doi.org/10.1172/jci72267

[21] Haffner, C., Dettmer, U., Weiler, T., Haass, C. (2007). The Nicastrin-like Protein Nicalin Regulates Assembly and Stability of the Nicalin-Nodal Modulator (NOMO) Membrane Protein Complex Journal of Biological Chemistry 282(14), 10632-10638. https://dx.doi.org/10.1074/jbc.m611033200

[22] Chen, Y., Kao, C., Chen, Y., Wang, C., Wu, C., Tsai, C., Liu, F., Yang, C., Wei, Y., Hsu, M., Tsai, S., Tsai, T. (2009). Cisd2 deficiency drives premature aging and causes mitochondria-mediated defects in mice Genes & Development 23(10), 1183-1194. https://dx.doi.org/10.1101/gad.1779509

[23] Camara, A., Zhou, Y., Wen, P., Tajkhorshid, E., Kwok, W. (2017). Mitochondrial VDAC1: A Key Gatekeeper as Potential Therapeutic Target Frontiers in Physiology 8(), 460. https://dx.doi.org/10.3389/fphys.2017.00460

[24] Perico, L., Conti, S., Benigni, A., Remuzzi, G. (2016). Podocyte–actin dynamics in health and disease Nature Reviews Nephrology 12(11), 692-710. https://dx.doi.org/10.1038/nrneph.2016.127

[25] Jeong, J., Kim, K., Lim, D., Kim, K., Kim, H., Lee, S., Song, J., Moon, B., Choy, H., Park, S. (2017). Microvasculature remodeling in the mouse lower gut during inflammaging Scientific Reports 7(1), 39848. https://dx.doi.org/10.1038/srep39848

[26] Zhou, L., Li, Y., Zhou, D., Tan, R., Liu, Y. (2013). Loss of Klotho Contributes to Kidney Injury by Derepression of Wnt/β-Catenin Signaling Journal of the American Society of Nephrology 24(5), 771-785. https://dx.doi.org/10.1681/asn.2012080865

[27] Kuro-o, M., Matsumura, Y., Aizawa, H., Kawaguchi, H., Suga, T., Utsugi, T., Ohyama, Y., Kurabayashi, M., Kaname, T., Kume, E., Iwasaki, H., Iida, A., Shiraki-Iida, T., Nishikawa, S., Nagai, R., Nabeshima, Y. (1997). Mutation of the mouse klotho gene leads to a syndrome resembling ageing Nature 390(6655), 45-51. https://dx.doi.org/10.1038/36285

[28] Kurosu, H., Yamamoto, M., Clark, J., Pastor, J., Nandi, A., Gurnani, P., McGuinness, O., Chikuda, H., Yamaguchi, M., Kawaguchi, H., Shimomura, I., Takayama, Y., Herz, J., Kahn, C., Rosenblatt, K., Kuro-o, M. (2005). Suppression of Aging in Mice by the Hormone Klotho Science 309(5742), 1829-1833. https://dx.doi.org/10.1126/science.1112766

[29] Vallon, V., Platt, K., Cunard, R., Schroth, J., Whaley, J., Thomson, S., Koepsell, H., Rieg, T. (2011). SGLT2 Mediates Glucose Reabsorption in the Early Proximal Tubule Journal of the American Society of Nephrology 22(1), 104-112. https://dx.doi.org/10.1681/asn.2010030246

[30] Flurkey, K., Astle, C., Harrison, D. (2010). Life Extension by Diet Restriction and N-Acetyl-L-Cysteine in Genetically Heterogeneous Mice The Journals of Gerontology: Series A 65A(12), 1275-1284. https://dx.doi.org/10.1093/gerona/glq155

[31] Zachos, N., Li, X., Kovbasnjuk, O., Hogema, B., Sarker, R., Lee, L., Li, M., Jonge, H., Donowitz, M. (2009). NHERF3 (PDZK1) Contributes to Basal and Calcium Inhibition of NHE3 Activity in Caco-2BBe Cells Journal of Biological Chemistry 284(35), 23708-23718. https://dx.doi.org/10.1074/jbc.m109.012641

[32] Lanaspa, M., Giral, H., Breusegem, S., Halaihel, N., Baile, G., Catalán, J., Carrodeguas, J., Barry, N., Levi, M., Sorribas, V. (2007). Interaction of MAP17 with NHERF3/4 induces

translocation of the renal Na/Pi IIa transporter to the trans -Golgi American Journal of Physiology-Renal Physiology 292(1), F230-F242. https://dx.doi.org/10.1152/ajprenal.00075.2006

[33] Tang, Y., Horikawa, I., Ajiro, M., Robles, A., Fujita, K., Mondal, A., Stauffer, J., Zheng, Z., Harris, C. (2013). Downregulation of splicing factor SRSF3 induces p53β, an alternatively spliced isoform of p53 that promotes cellular senescence Oncogene 32(22), 2792-2798. https://dx.doi.org/10.1038/onc.2012.288

[34] Robinson, W. (2009). Ecological Correlations and the Behavior of Individuals International Journal of Epidemiology 38(2), 337-341. https://dx.doi.org/10.1093/ije/dyn357

[35] Anisimova, A., Meerson, M., Gerashchenko, M., Kulakovskiy, I., Dmitriev, S., Gladyshev, V. (2020). Multifaceted deregulation of gene expression and protein synthesis with age Proceedings of the National Academy of Sciences 117(27), 15581-15590. https://dx.doi.org/10.1073/pnas.2001788117

[36] Cellerino, A., Ori, A. (2017). What have we learned on aging from omics studies? Seminars in Cell & Developmental Biology 70(), 177-189. https://dx.doi.org/10.1016/j.semcdb.2017.06.012

[37] Lake, B., Chen, S., Hoshi, M., Plongthongkum, N., Salamon, D., Knoten, A., Vijayan, A., Venkatesh, R., Kim, E., Gao, D., Gaut, J., Zhang, K., Jain, S. (2019). A single-nucleus RNA-sequencing pipeline to decipher the molecular anatomy and pathophysiology of human kidneys Nature Communications 10(1), 2832. https://dx.doi.org/10.1038/s41467-019-10861-2

[38] Gisler, S., Pribanic, S., Bacic, D., Forrer, P., Gantenbein, A., Sabourin, L., Tsuji, A., Zhao, Z., Manser, E., Biber, J., Murer, H. (2003). PDZK1: I. A major scaffolder in brush borders of proximal tubular cells 1 1 See Editorial by Moe, p. 1916. Kidney International 64(5), 1733-1745. https://dx.doi.org/10.1046/j.1523-1755.2003.00266.x

[39] Giral, H., Lanzano, L., Caldas, Y., Blaine, J., Verlander, J., Lei, T., Gratton, E., Levi, M. (2011). Role of PDZK1 Protein in Apical Membrane Expression of Renal Sodium-coupled Phosphate Transporters Journal of Biological Chemistry 286(17), 15032-15042. https://dx.doi.org/10.1074/jbc.m110.199752

[40] Liu, Y., Beyer, A., Aebersold, R. (2016). On the Dependency of Cellular Protein Levels on mRNA Abundance Cell 165(3), 535-550. https://dx.doi.org/10.1016/j.cell.2016.03.014

[41] Labbadia, J., Morimoto, R. (2014). The Biology of Proteostasis in Aging and Disease Annual Review of Biochemistry 84(1), 1-30. https://dx.doi.org/10.1146/annurev-biochem-060614-033955

[42] Gerdes Gyuricza et al., companion paper

[43] Morgan, A., Fu, C., Kao, C., Welsh, C., Didion, J., Yadgary, L., Hyacinth, L., Ferris, M., Bell, T., Miller, D., Giusti-Rodriguez, P., Nonneman, R., Cook, K., Whitmire, J., Gralinski, L., Keller, M., Attie, A., Churchill, G., Petkov, P., Sullivan, P., Brennan, J., McMillan, L., Villena, F. (2016). The Mouse Universal Genotyping Array: From Substrains to Subspecies G3: Genes|Genomes|Genetics 6(2), 263 - 279. https://dx.doi.org/10.1534/g3.115.022087

[44] Broman, K., Gatti, D., Svenson, K., Sen, Ś., Churchill, G. (2019). Cleaning Genotype Data from Diversity Outbred Mice G3: Genes, Genomes, Genetics 9(5), g3.400165.2019. https://dx.doi.org/10.1534/g3.119.400165

[45] Raghupathy, N., Choi, K., Vincent, M., Beane, G., Sheppard, K., Munger, S., Korstanje, R., Villena, F., Churchill, G. (2018). Hierarchical analysis of RNA-seq reads improves the accuracy of allele-specific expression. Bioinformatics (Oxford, England) 34(13), 2177 - 2184. https://dx.doi.org/10.1093/bioinformatics/bty078

[46] Chick, J., Munger, S., Simecek, P., Huttlin, E., Choi, K., Gatti, D., Raghupathy, N., Svenson, K., Churchill, G., Gygi, S. (2016). Defining the consequences of genetic variation on a proteome-wide scale Nature 534(7608), 500-505. https://dx.doi.org/10.1038/nature18270

[47] Chikina, M., Zaslavsky, E., Sealfon, S. (2015). CellCODE: a robust latent variable approach to differential expression analysis for heterogeneous cell populations Bioinformatics 31(10), 1584-1591. https://dx.doi.org/10.1093/bioinformatics/btv015

[48] Conover, J. (1999). Practical Nonparemetric Statistics Wiley series in probability and statistics

Figure 1

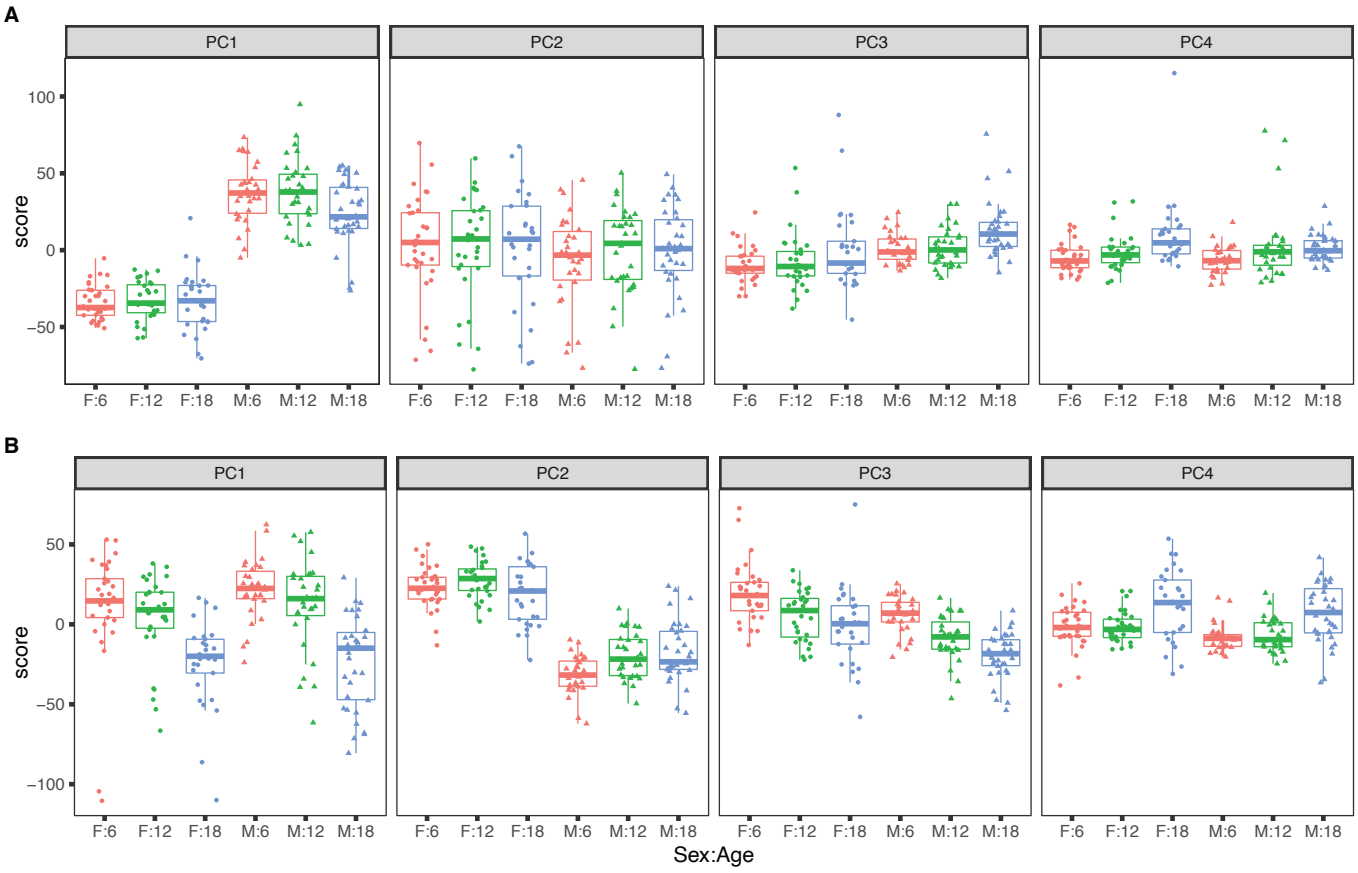

Figure 2

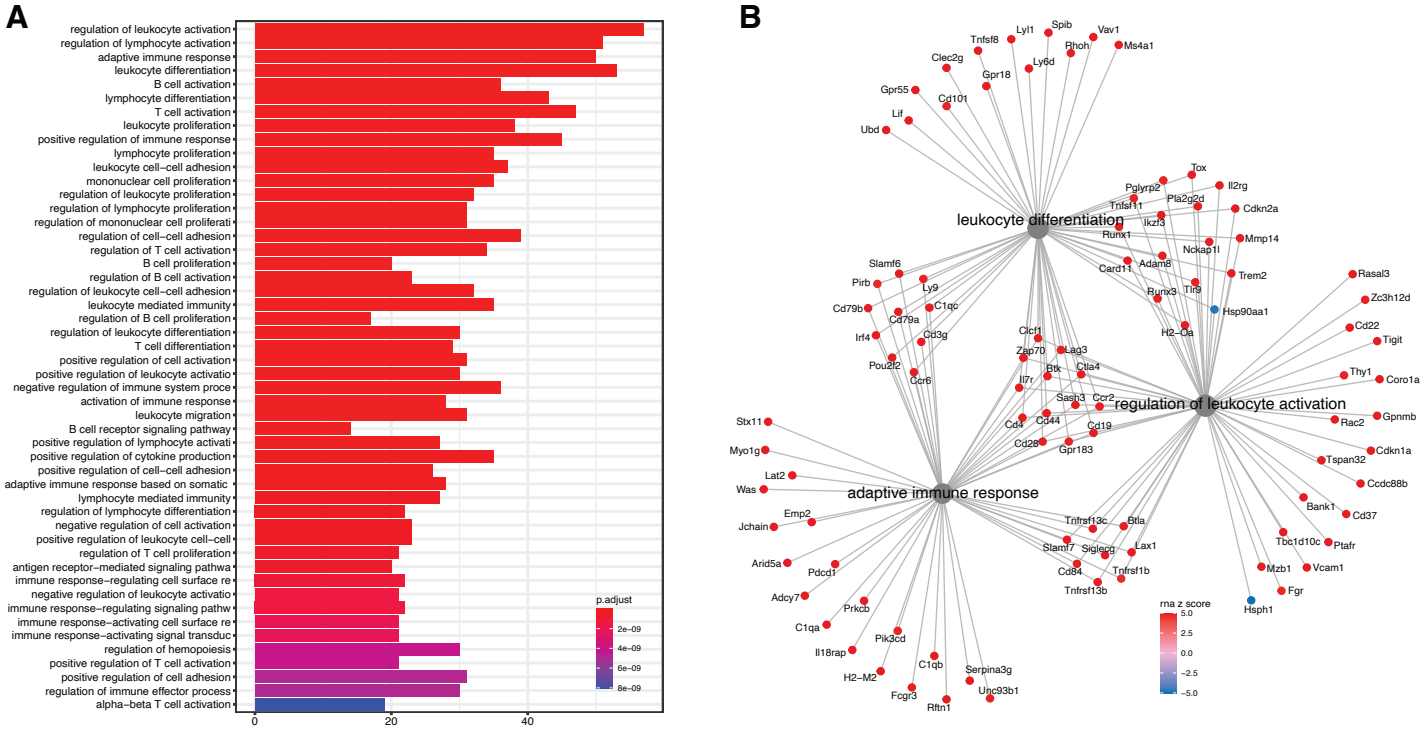

Figure 3

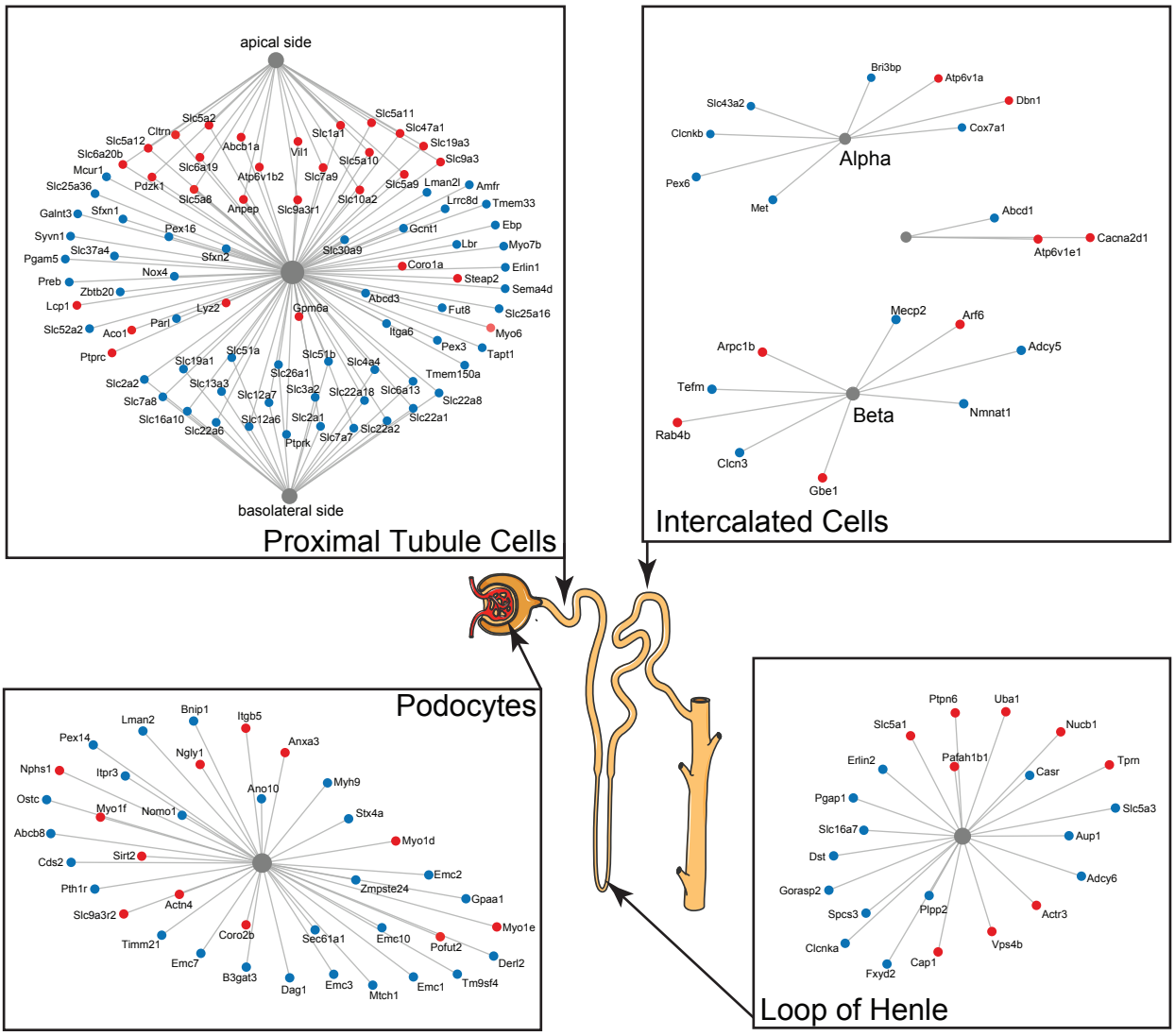

Figure 4

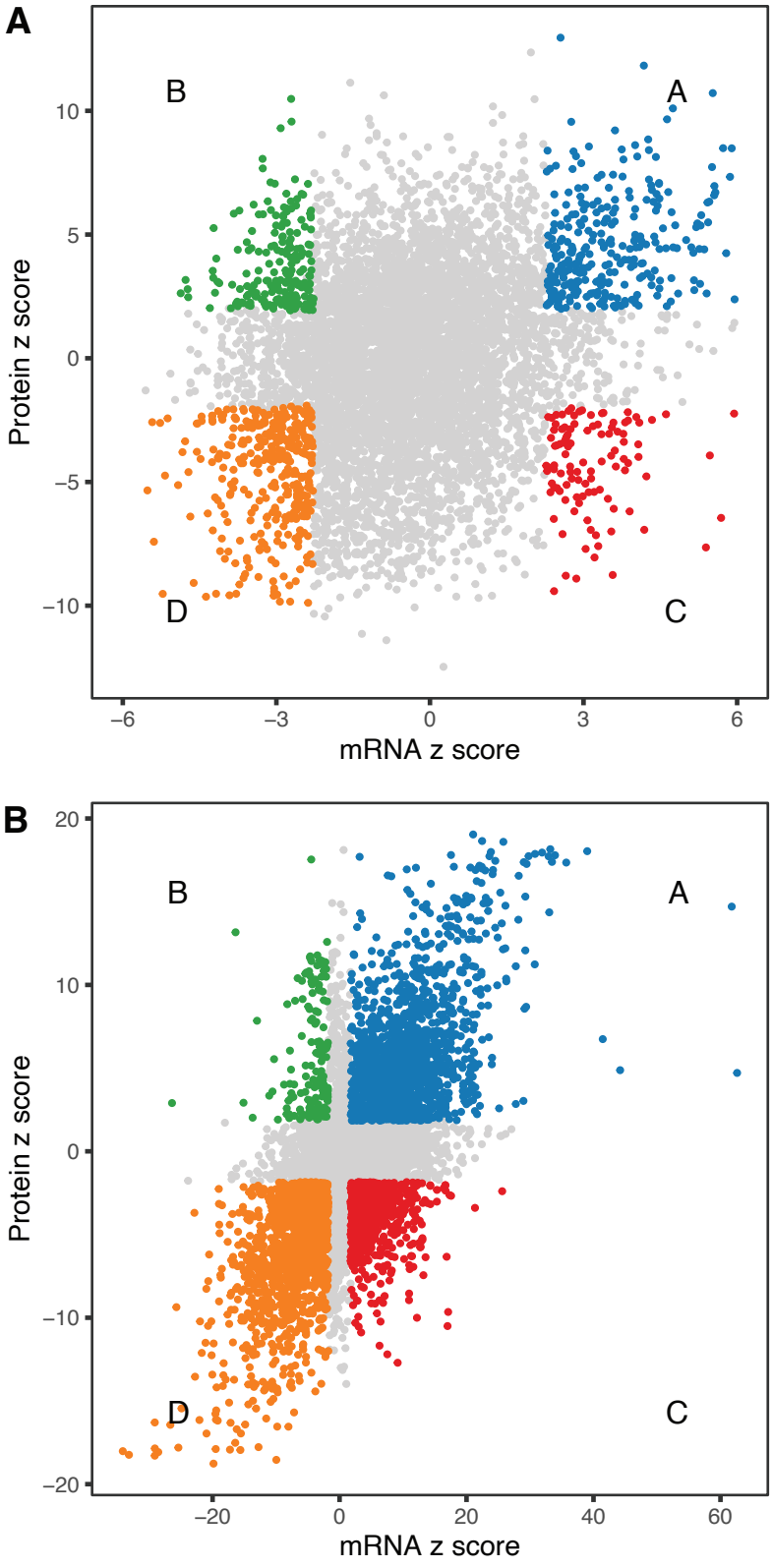

Figure 5

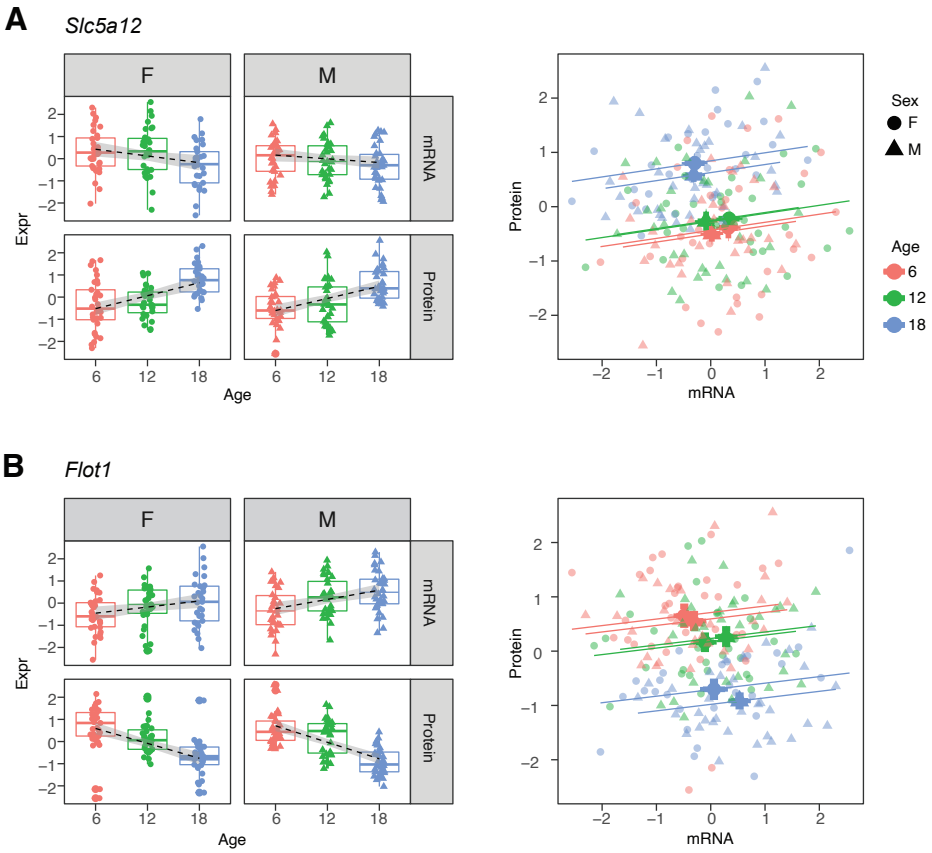

Figure 6

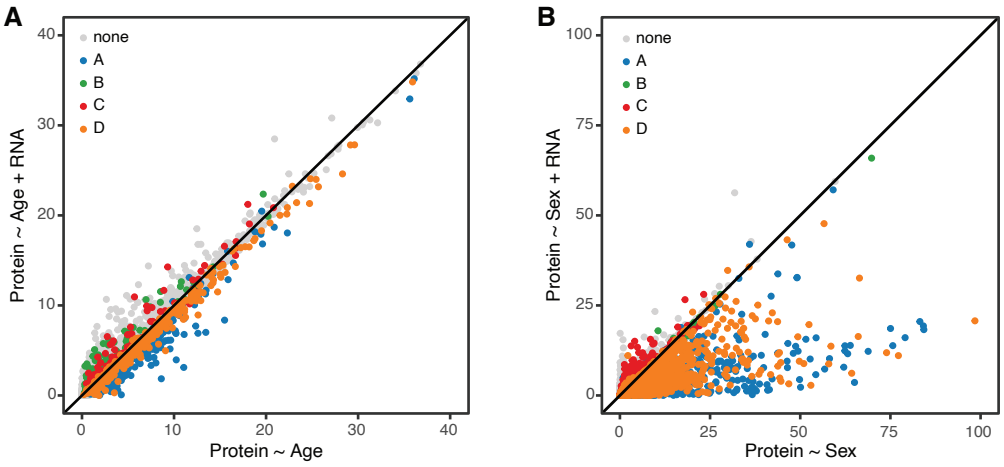

Figure 7

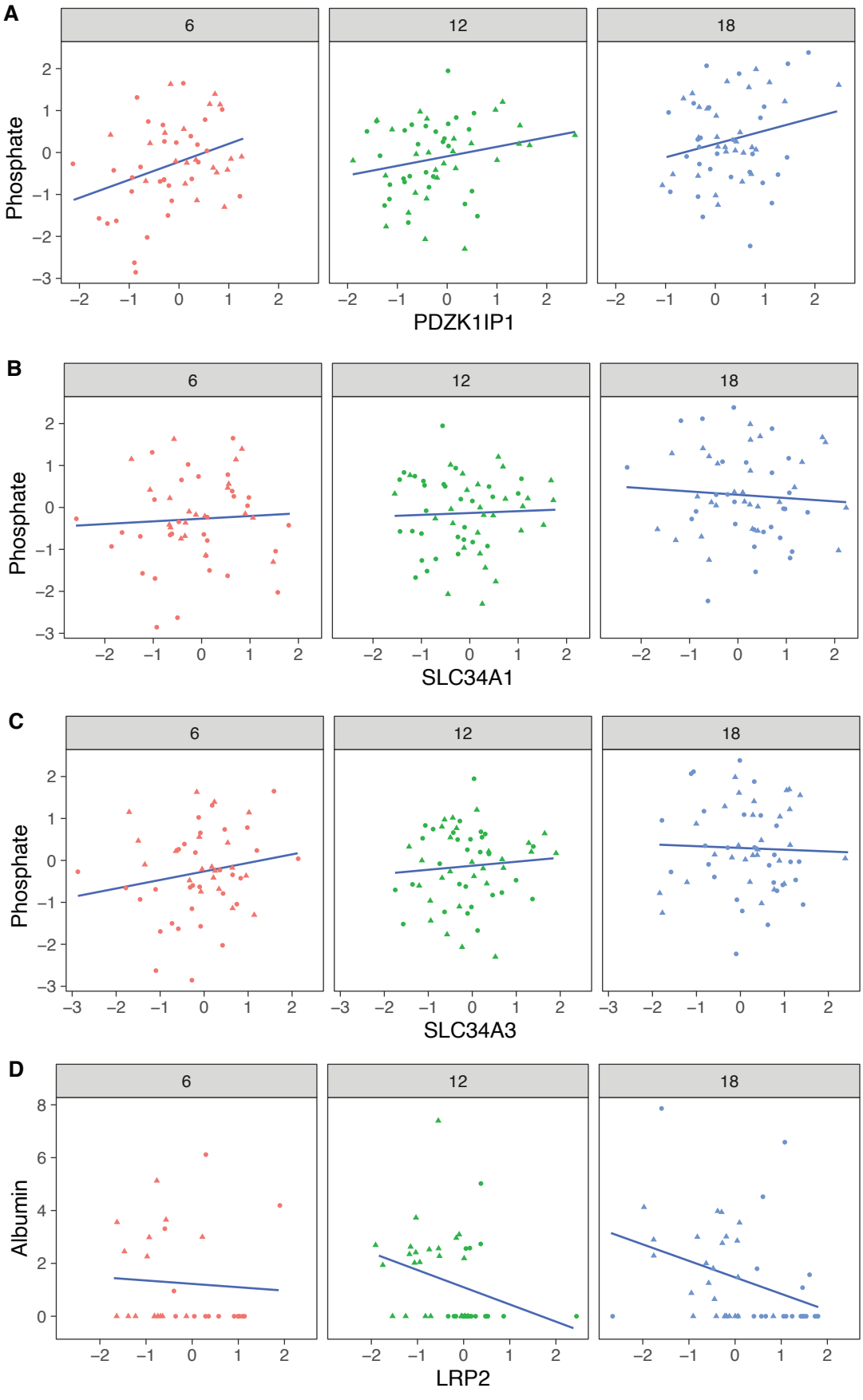

Figure 8

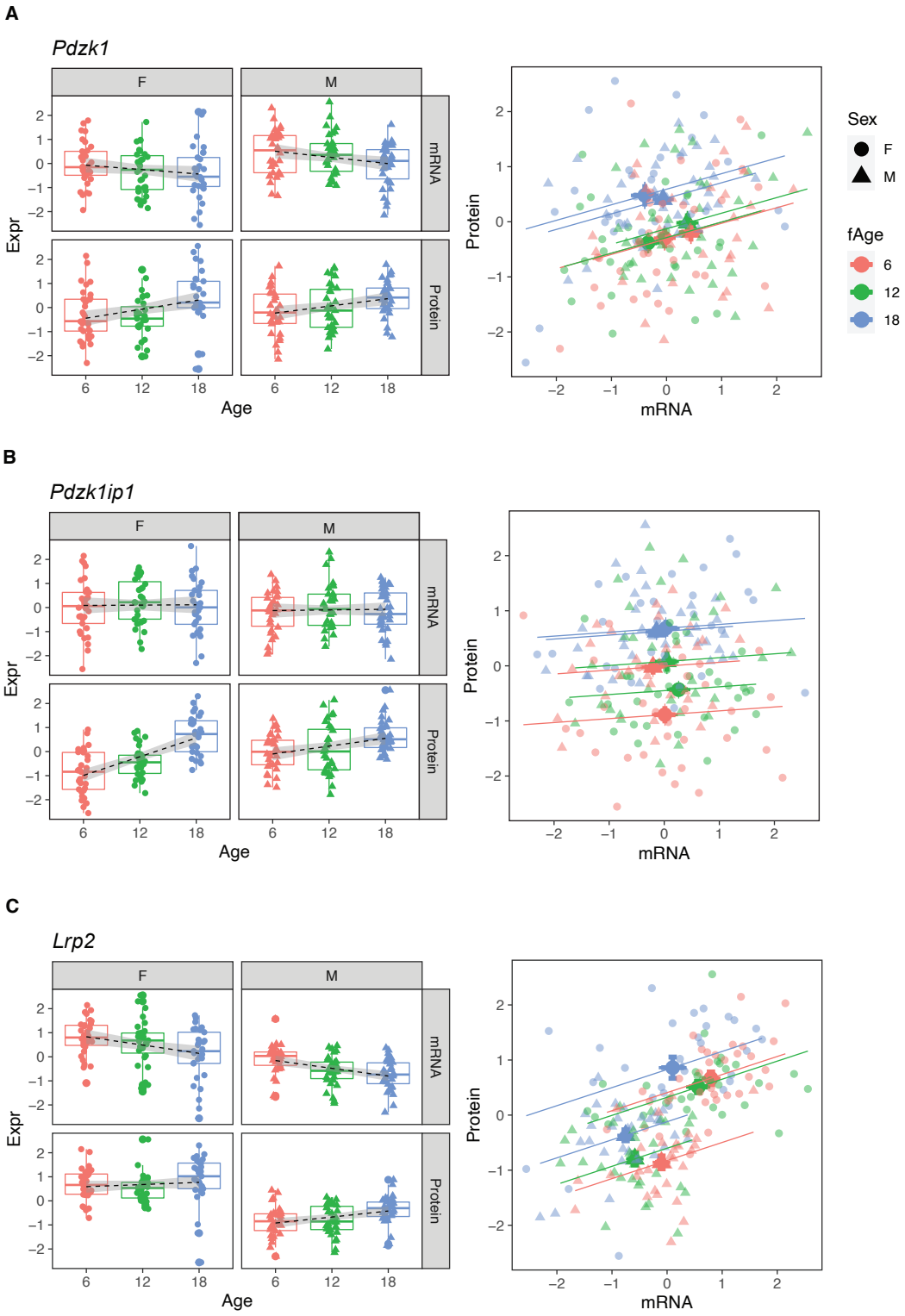

Figure S1

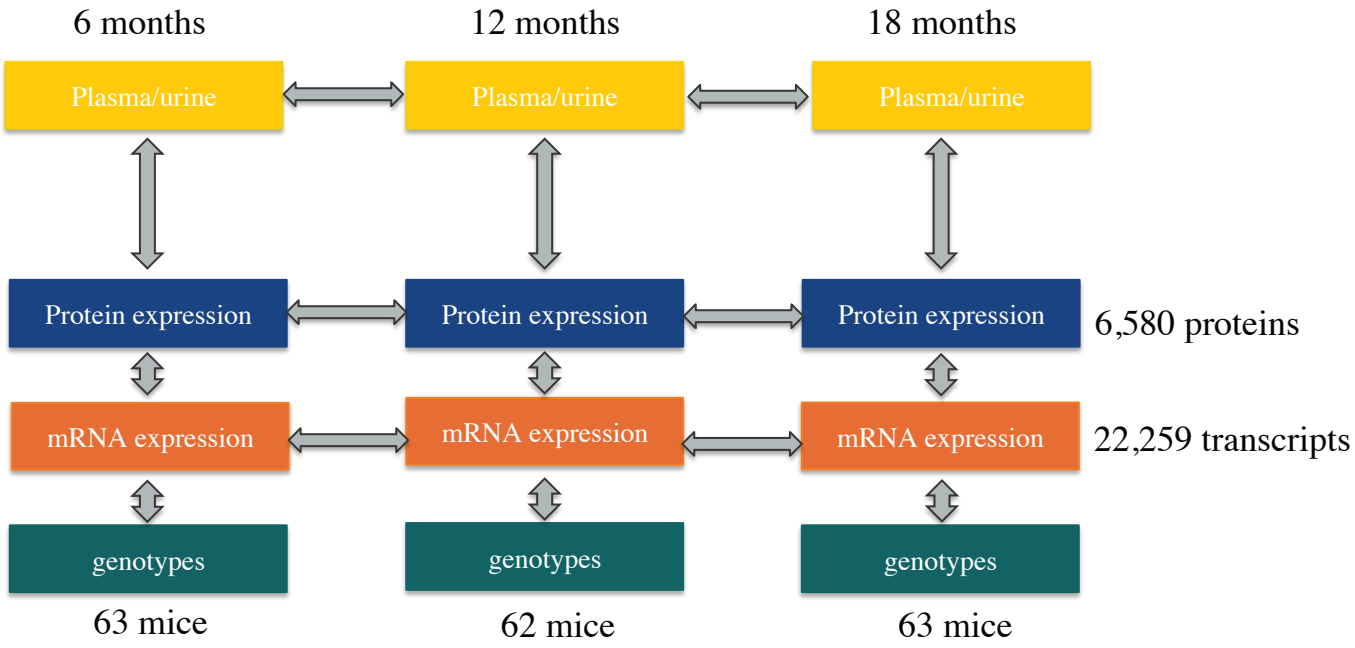

Figure S2

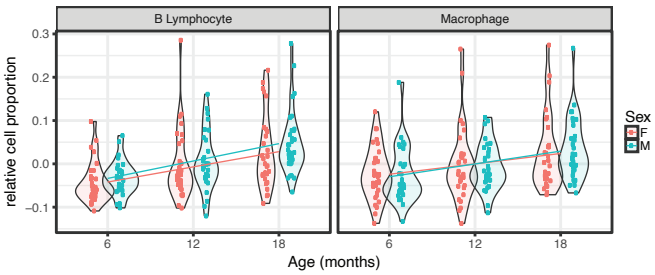

Figure S3

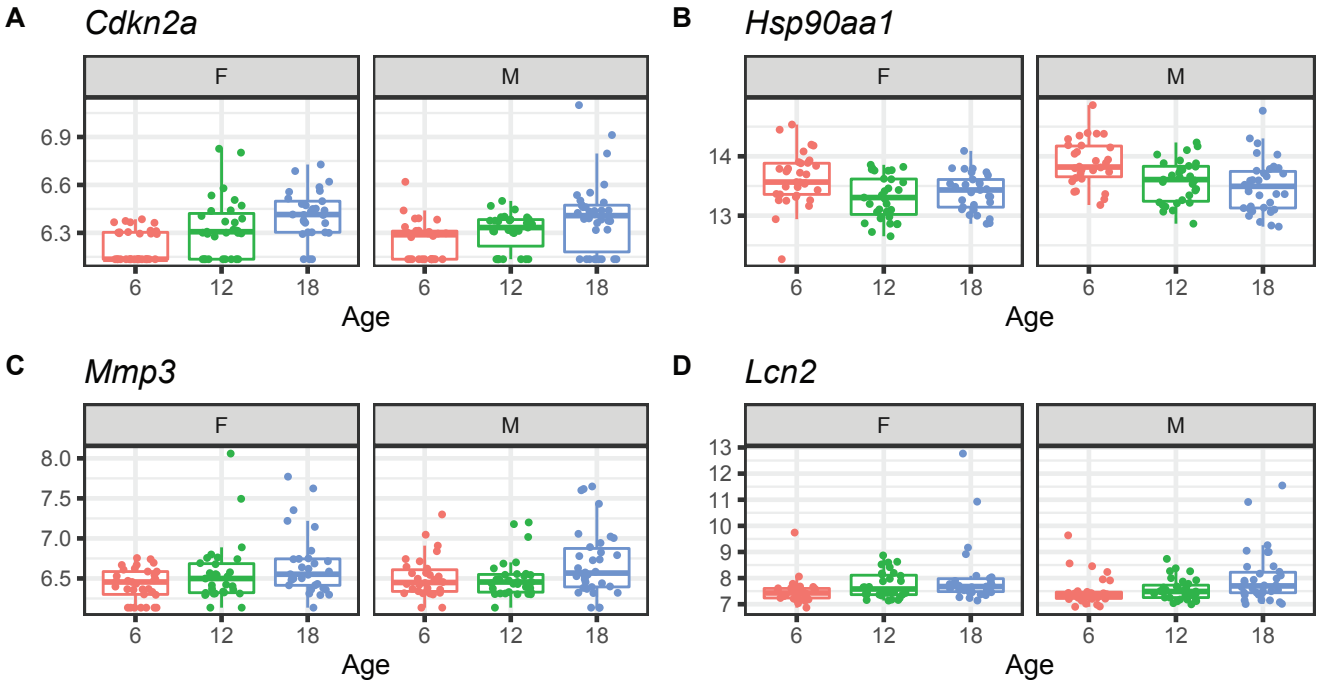

Figure S4

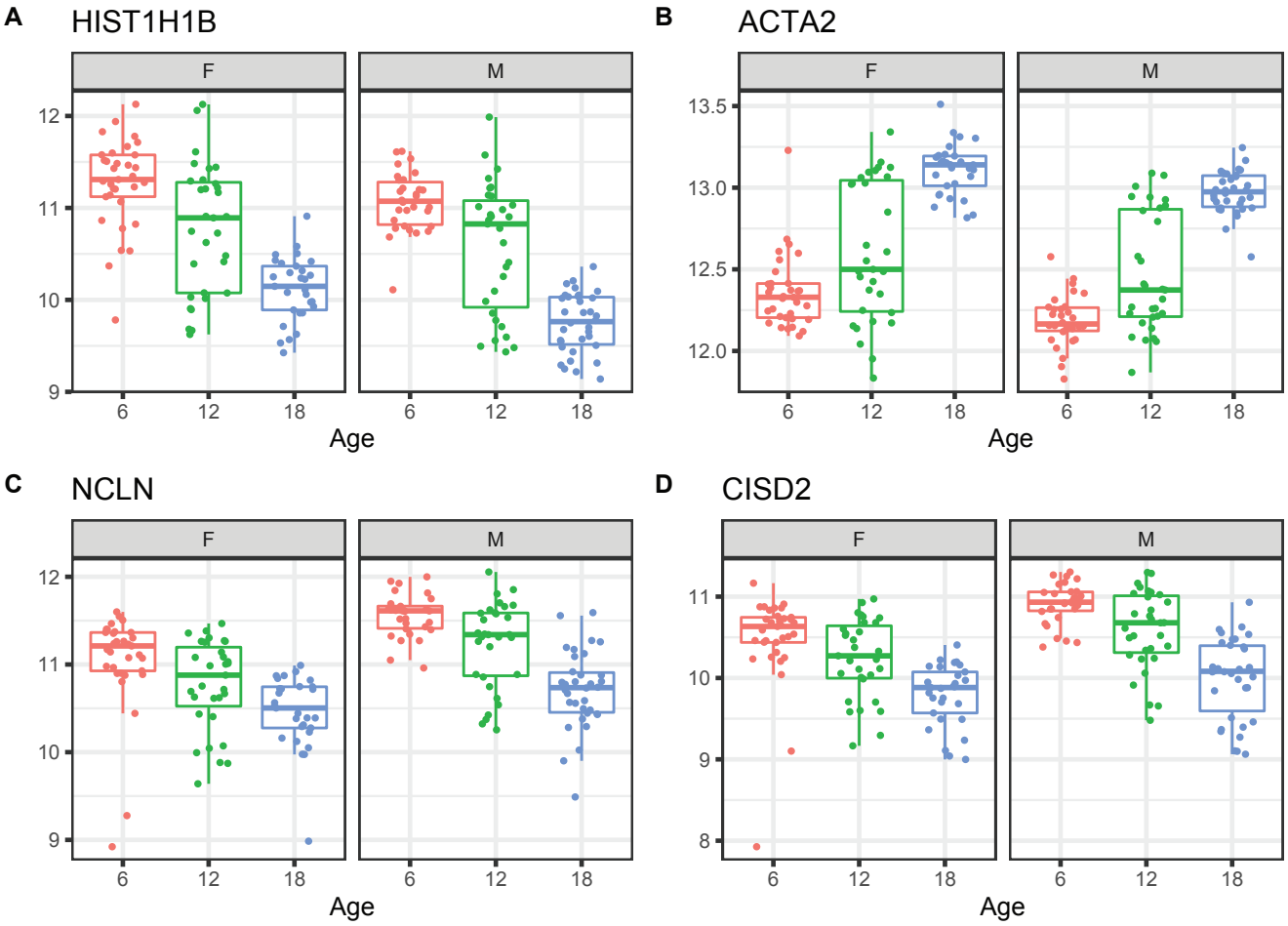

Figure S5